Archives of Materials Science and Engineering

Volume 111
Issue 1
September 2021
Pages 34-41

International Scientific Journal
published monthly by the
World Academy of Materials
and Manufacturing Engineering

DOI: 10.5604/01.3001.0015.5563

Mathematical forecasting composition of secondary carbides in the single-crystal superalloys

O.A. Glotka *, V.I. Olshanetskii

Zaporizhzhia Polytechnic National University, 64 Zhukovskogo str., 69063, Zaporizhzhia, Ukraine
* Corresponding e-mail address: Glotka-alexander@ukr.net
ORCID identifier: https://orcid.org/0000-0002-3117-2687 (O.A.G.);
https://orcid.org/0000-0002-9485-4896 (V.I.O.)

ABSTRACT

Purpose: Predicting the specifics of the distribution of alloying elements between secondary carbides, their topology, and morphology, as well as the composition for a single-crystal multicomponent system of the type Ni-11.5Cr-5Co-3.6Al-4.5Ti-7W-0.8Mo-0.06C using the calculated CALPHAD (passive experiment) versus scanning electron microscopy (active experiment).

Design/methodology/approach: This work presents the results of studies of the distribution of chemical elements in the composition of carbides, depending on their content in the system. The studies were carried out using an electron microscope with computer analysis of images and chemical composition.

Findings: It was found that the influence of alloying elements on the composition of carbides is complex and is described by complex dependencies that correlate well with the obtained experimental results.

Research limitations/implications: An essential problem is the prediction of the structure and properties of superalloys without or with a minimum number of experiments.

Practical implications: The obtained dependencies can be used both for designing new superalloys and for improving the compositions of industrial alloys.

Originality/value: The value of this work is that the obtained dependences of the influence of alloying elements on the dissolution (precipitation) temperatures and the distribution of elements in secondary carbides in the superalloy of the Ni-11.5Cr-5Co-3.6Al-4.5Ti-7W-0.8Mo-0.06C system. It was found that changes in the course of the curves of temperature dependence on the element content closely correlate with thermodynamic processes occurring in the system, that is, the curves exhibit extrema accompanying the change in the stoichiometry of carbides or the precipitation of new phases.

Keywords: Single-crystal nickel-based superalloys, Alloying system, CALPHAD method, Structure, Composition of secondary carbides

Reference to this paper should be given in the following way:

O.A. Glotka, V.I. Olshanetskii, Mathematical forecasting composition of secondary carbides in the single-crystal superalloys, Archives of Materials Science and Engineering 111/1 (2021) 34-41. DOI: https://doi.org/10.5604/01.3001.0015.5563

METHODOLOGY OF RESEARCH, ANALYSIS AND MODELLING

1. Introduction

The advantage of single-crystal alloys in comparison with polycrystalline alloys is a significantly higher resistance to high-temperature creep, due to the absence of grain boundaries in the alloy, since their structure is formed by branches of a single dendrite developed from a single-crystal seed. This dendrite permeates the entire single crystal with many branches of the first and second orders. The first-order axes of the dendrite grow along with the directional heat flow that is created in the directional solidification furnace and coincides with the longitudinal axis of the single-crystal blade. At the microscopic level, the structure of single-crystal nickel-based superalloys is represented by only two phases: particles of the γ′-phase (formed based on the intermetallic compound Ni_3Al - an ordered fcc structure of the L_12 type), scattered in a matrix from a γ-solid solution of alloying elements in nickel (disordered fcc – structure). However, there is a class of materials with the addition of carbon in small amounts (up to 0.1 wt.%), which leads to the appearance of a carbide phase in the structure of alloys [1-13].

The role of carbides is very complex in nickel-based superalloys. They affect mechanical properties depending on their morphology and distribution. Single-crystal alloys are characterized by the presence of primary carbides of spherical, block, or font morphology, as well as secondary carbides of discontinuous block or lamellar morphology [14-19]. The main methods for studying such fine structures are X-ray spectroscopy, which fully makes it possible to determine the main characteristics [20-23].

This work aims to study the possibility of predicting the specifics of the distribution of alloying elements between secondary carbides, their topology, and morphology, as well as the composition for a single-crystal multicomponent system of the type Ni-11.5Cr-5Co-3.6Al-4.5Ti-7W-0.8Mo-0.06C using the calculation method CALPHAD (passive experiment) compared with the data obtained by scanning electron microscopy (active experiment).

2. Materials and test methods

Modelling of thermodynamic processes occurring during crystallization (cooling) or heating in the structure of alloys was carried out by the CALPHAD method [24].

Modelling of these processes allows for computational prediction and comparative assessment of the effect of alloying elements in different types of carbides on their distribution and phase composition in the alloys under study. Calculations were carried out for each investigated composition individually with the stepwise introduction of a specific alloying element into a fixed composition of a multi-component system.

Depending on the alloying system of the alloy, the results obtained by modelling the crystallization process make it possible to calculate the temperatures and the number of precipitated types of carbides, as well as their chemical composition.

In the multicomponent alloying system (Ni-11.5Cr-5Co-3.6Al-4.5Ti-7W-0.8Mo-0.06C), the range of variation of the elements was chosen from considerations of the maximum and minimum amount of the element introduced into the superalloys. Thus, for the study were selected carbide-forming elements in the following alloying ranges: carbon (0.02-0.2)%; chromium (1-35)%; molybdenum (0.5-6)%; tungsten (1-16)% by weight.

The alloy crystallization process was simulated from the temperature of the liquid state (1600°C) to room temperature (20°C) with a temperature step of 10°C over the entire range, which made it possible to determine the temperature sequence of phase precipitation during the crystallization process.

Predictive calculations were carried out based on the initial chemical composition of the alloy with the determination of the most probable precipitation of the amount and type of carbides in the structure, as well as their chemical composition after modelling the crystallization process.

The composition of carbides was experimentally determined using a REM-106I scanning electron microscope with an X-ray spectral microanalysis system. This method was used to study morphology and chemical composition of precipitated carbides in the alloy structure. The conversion of qualitative values into quantitative analysis was carried out automatically according to the program of the device. The relative error of the method is ±1% (by weight). The results of calculations of the type of carbides and their chemical composition were compared with the experimental data obtained using electron microscopy.

The obtained dependences have rather high coefficients of determination $R^2 \geq 0.9$ and can be used for predictive calculations of the indicated characteristics with a relative error of ± 3.1%.

3. Influence of elements on the phase composition of the composition

The study of phase separation during crystallization of the investigated alloy in the temperature range (1600–20°C) showed that the most probable is the separation of the main

phases in the following order: γ – solid solution; primary carbides; eutectic γ + γ′; type γ′ intermetallic based on (Ni_3Al). Carbides $M_{23}C_6$ are formed in alloys with moderate or high chromium content during low-temperature processing and during operation at 760-980°C due to the decomposition of MC carbides and from the "residual" carbon dissolved in the matrix. They are usually located along grain boundaries, sometimes along twin lines, at stacking faults, and at the ends of twins, and can be nucleation centres for σ-phase plates. The main elements that make up their composition are chromium, molybdenum, and tungsten, in this regard, in the future, modelling and experimental study of the distribution of these elements is carried out.

It was found that the dependence of the amount of $M_{23}C_6$ carbides on the carbon content is linear and is optimally described by the formulas (Tab. 1), which are shown in Figure 1. Carbon does not affect the temperature of dissolution (precipitation) of secondary carbides, which is at the level of 1025±10°C.

Chromium, one of the main elements that enhance the corrosion resistance characteristics of modern industrial nickel-based superalloys. On average, the chromium content is at the level of 15% by wt., however, to increase the heat resistance, its amount can be raised to 35% by wt. [25]. In addition to its corrosive properties, chromium participates in the formation of one of the secondary carbides of the $M_{23}C_6$ type. It was found that the effect of the amount of chromium on the temperature of dissolution (precipitation) and the composition of secondary carbides (Fig. 2) is complex and is described by the following formulas (Tab. 1).

Table 1.
Dependences of the temperature of dissolution (precipitation) of carbides and the content of alloying elements in secondary carbides on the content of alloying elements in the alloy

Alloying element	Dissolution (precipitation) temperatures of carbides, °C	Content of elements in carbide, wt.%
C	-	$V_{M23C6} = 20{,}239(C)\text{-}0{,}0013$
Cr	$t_L^{M23C6}, °C = 0.0262\cdot(C_{Cr})^3\text{-}2.1506\ (C_{Cr})^2 + 58.267(C_{Cr}) + 568.34$	$C_{Cr} = -0.0665(C_{Cr}\text{ in alloy})^2 + 3.7149(C_{Cr}\text{ in alloy}) + 31.847$; $C_{Mo} = -0.0348(C_{Cr}\text{ in alloy})^2 - 1.9008(C_{Cr}\text{ in alloy}) + 27.249$; $C_W = 1.245(C_{Cr}\text{ in alloy}) - 3.965$ (from 9 to 15% Cr)
Mo	$t_L^{M23C6}, °C = 14{,}37\ln(C_{Mo}) + 1030.6$	$C_{Mo} = 5.4835\ \ln(C_{Mo}\text{ in alloy}) + 8{,}6222$; $C_W = -6.237\ \ln(C_{Mo}\text{ in alloy}) + 12.493$; $C_{Ni} = -0.0455(C_{Mo}\text{ in alloy})^2 + 0.7416(C_{Mo}\text{ in alloy}) + 4.5485$
W	$t_L^{M23C6}, °C = 4.1647\ (C_W) + 994.85$	$C_W = -0.0999(C_W\text{ in alloy})^2 + 2.8216(C_W\text{ in alloy}) - 1.8997$; $C_{Mo} = 0.0193(C_W\text{ in alloy})^2 - 1.2152(C_W\text{ in alloy})\ 15.488$; $C_{Ni} = 0.0499(C_W\text{ in alloy})^2 - 1.3375(C_W\text{ in alloy}) + 11.587$

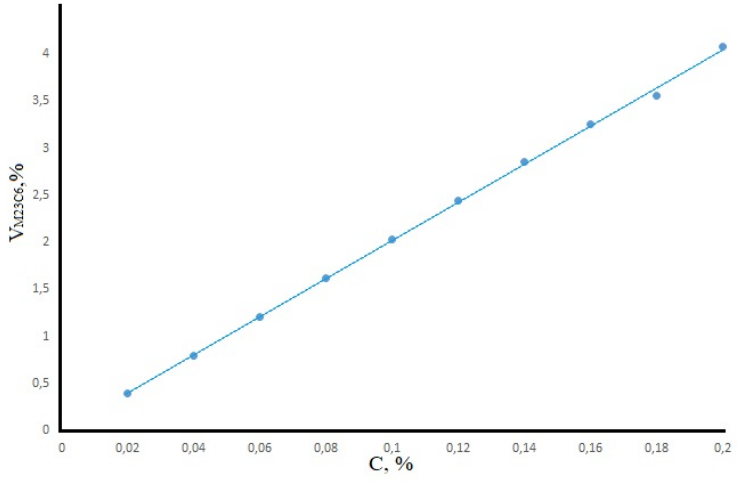

Fig. 1. Dependence of the number of secondary carbides $M_{23}C_6$ on the carbon content in the alloy composition

A decrease in the rate of increase in the temperature of dissolution (precipitation) of secondary carbides is observed after reaching the amount of chromium in the alloy of more than 19%, which is explained by the precipitation of a topologically close-packed (TCP) P-phase in the alloy, which has the composition 55.2W-19.6Cr-14.2Ni-6.6Mo-4.2Co. Also, at 19% chromium in the alloy, the amount of tungsten in the secondary carbide abruptly decreases to 6.8% and practically does not change (Fig. 2b). An increase in chromium in the alloy by more than 23% leads to the termination of its dissolution in the matrix and the precipitation of a α-chromium-based solid solution.

Molybdenum, one of the elements that participate in the formation of secondary carbides, and on its basis carbides of the M_6C type can be formed, while molybdenum can be included in the composition of carbides of the $M_{23}C_6$ type [26].

Figure 3 shows that molybdenum has a complex effect not only on the temperature of dissolution (precipitation) of secondary carbides but also affects the chemical composition of carbides.

The influence of molybdenum is ambiguous on the temperatures of formation of carbides (carbide liquidus), according to the logarithmic dependence (Tab. 1), (Fig. 3a).

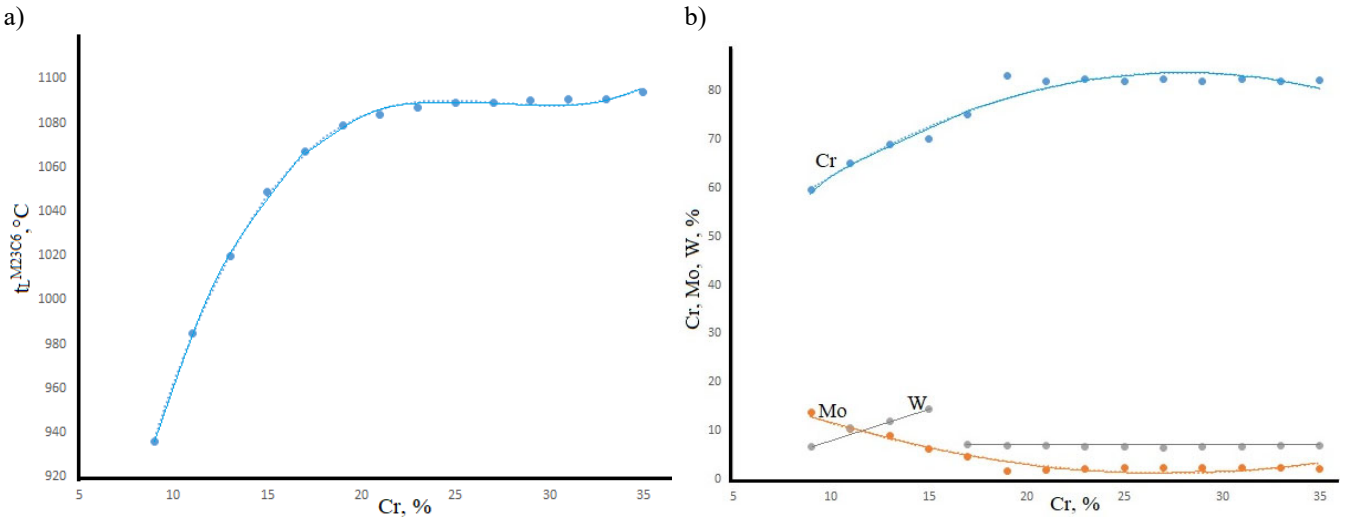

Fig. 2. Effect of the chromium content in the alloy on the temperature of dissolution (precipitation) of carbides of the $M_{23}C_6$ type (a), the amount of chromium, molybdenum, and tungsten in the secondary carbide (b)

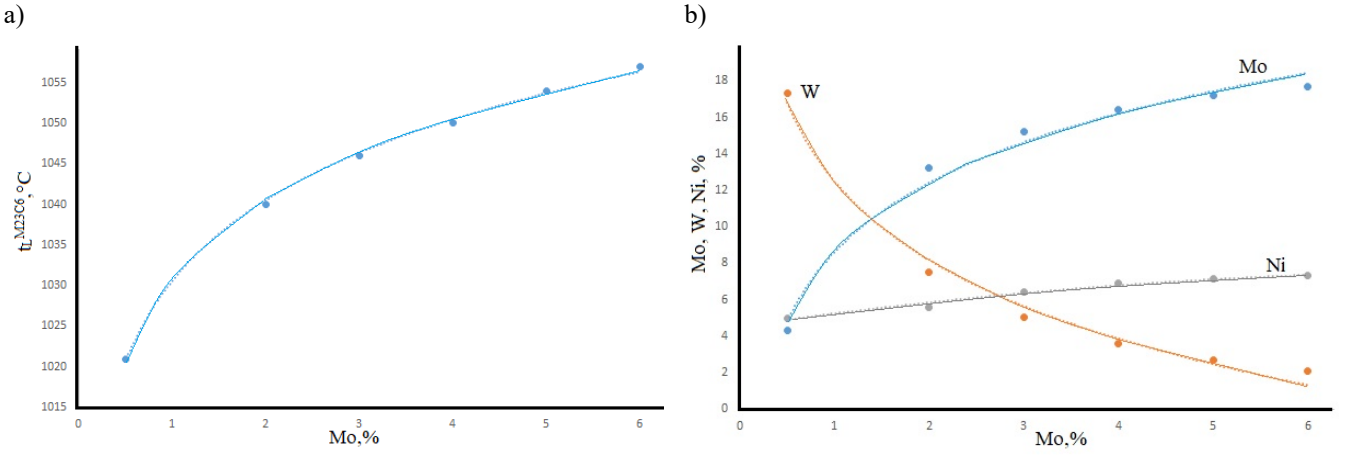

Fig. 3. Influence of the content of molybdenum in the composition of the alloy on the temperature of dissolution (precipitation) carbides $M_{23}C_6$ type (a), the amount of molybdenum, tungsten, and nickel in the secondary carbide (b)

It should be noted that molybdenum rapidly increases in the composition of secondary carbides, and at a concentration (2%), the content of tungsten in carbides predominates (Fig. 3b). Also, at a concentration of 2% Mo in the alloy, a P-phase enriched in tungsten is formed. An increase in the molybdenum content up to 5% leads to the formation carbide of the M_6C type, which contains a significant portion of Mo.

Tungsten is introduced into the composition of heat-resistant alloys to increase the level of temperatures of phase transformations, and, consequently, the superalloy. The tungsten content in modern heat-resistant alloys is within a fairly wide range of 1-16% by weight. A further increase in the tungsten content significantly increases the probability of precipitation of phases [27-30] in the TCP structure. An increase in the concentration of tungsten in the alloy leads to an increase in the temperature of dissolution (precipitation) of carbides $M_{23}C_6$ (Fig. 4a), this is explained by an increase in interatomic bonds in secondary precipitates. Thus, the tungsten content in $M_{23}C_6$ increases almost immediately and reaches a maximum of 9-11% tungsten in the alloy (Fig. 4b). At the same tungsten concentrations, the P-phase and carbides of the M_6C type are precipitated in the alloy, which may be the reason for the end of a further increase in the W content in the $M_{23}C_6$ carbides. The concentration of molybdenum and nickel in secondary carbides gradually decreases according to the corresponding parabolic dependences (Tab. 1).

4. Comparison of calculations and experimental data

The results of calculating the phase composition obtained by the CALPHAD method were further compared with the experimental data obtained using electron microscopy in the microprobe mode on a scanning electron microscope, REM-106I. Typical morphology of secondary carbides, which is most often found in the structure of alloys of this class: intermittent lamellar (Fig. 5a) and intermittent block (Fig. 5b). The most preferable is the block type of precipitates of secondary carbides since in this case, we have a lower level of stress concentration with the matrix. In single-crystal alloys containing carbon, secondary carbides are precipitated not along grain boundaries, but along phase boundaries (γ-γ′ eutectics and dendrites).

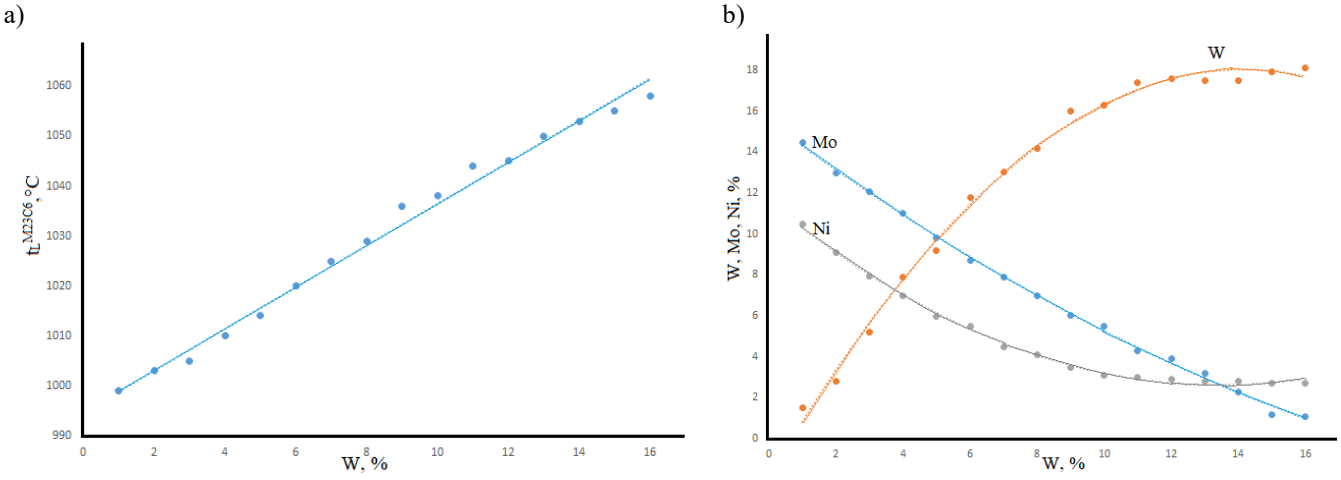

Fig. 4. Influence of the tungsten content in the alloy on the temperature of dissolution (precipitation) of carbides of the $M_{23}C_6$ type (a); the amount of molybdenum, tungsten, and nickel in the secondary carbide (b)

Table 2.
Change in the composition of secondary carbides in the alloy of the Ni-11.5Cr-5Co-3.6Al-4.5Ti-7W-0.8Mo-0.06C system

Method of obtaining results	Element content, % wt.					
	Cr	W	Mo	Ni	Co	C
Calculated	66.58	15.27	6.45	5.59	1.27	4.82
Experimental (Fig. 5, point 1)	61.68	12.38	13.07	6.61	1.41	4.82
Experimental (Fig. 5, point 1)	60.44	14.05	13.91	5.82	0.8	4.82

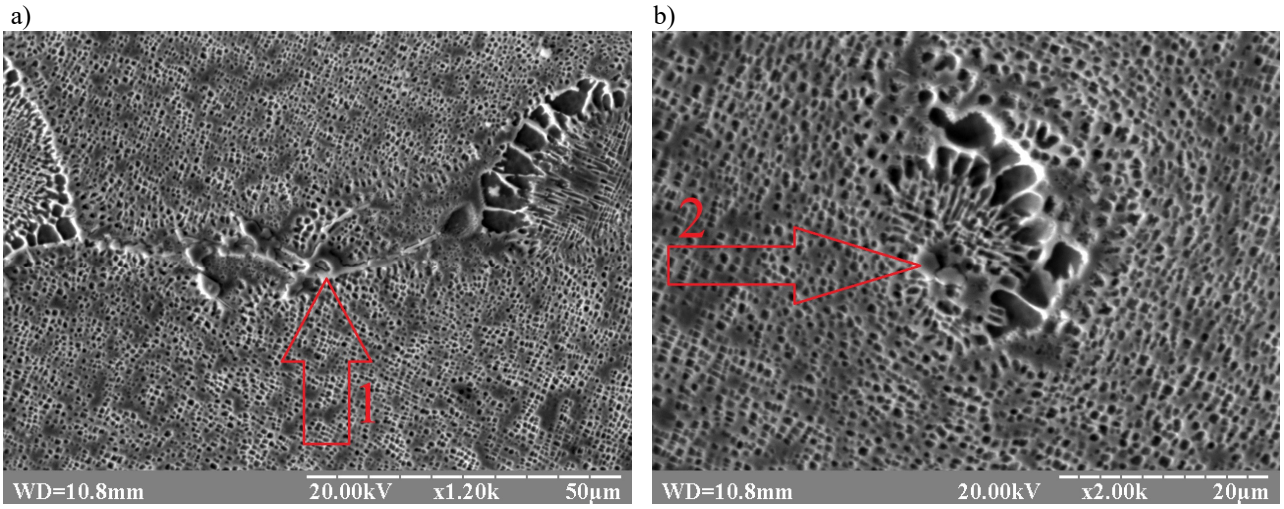

Fig. 5. Typical morphology of secondary carbides in the structure of a system Ni-11.5Cr-5Co-3.6Al-4.5Ti-7W-0.8Mo-0.06C

The chemical composition of carbides was determined experimentally by the method of X-ray spectral microanalysis, with the help of which the intensity of X-ray radiation was recorded as a function of the energy keV. It was experimentally established that the composition of carbides includes chromium, tungsten, molybdenum, cobalt, and nickel in the following ratios with the calculated values (Tab. 2). The errors in determining the elements by this method did not exceed ±3% by weight.

Table 2 shows that the calculated and experimental data are in good agreement with each other for almost all elements. There is a slight discrepancy in the content of chromium and molybdenum, due to possible measurement and calculation errors. Such a distribution of elements in carbides is typical for materials of this class and does not contradict well-known concepts.

Thus, the calculated data obtained by the CALPHAD method to determine the type and chemical composition of carbides showed good convergence and agreement with the experimental data obtained by electron microscopy.

5. Conclusions

Based on an integrated approach for the multicomponent system Ni-11.5Cr-5Co-3.6Al-4.5Ti-7W-0.8Mo-0.06C, new regression models have been obtained that make it possible to adequately predict the chemical composition of secondary carbides from the chemical composition of the alloy.

The dependences of the influence of alloying elements on the temperatures of dissolution (precipitation) of carbides have been established. It is shown that the contents of elements closely correlate with the thermodynamic processes occurring in the system, that is, the curves exhibit extrema accompanying the change in the stoichiometry of carbides.

It was found that with an increase in the chromium concentration over 19%, the P-phase is precipitated and the tungsten content in the secondary carbides decreases. At a chromium concentration of more than 23%, a α-chromium-based solid solution is formed in the alloy structure. The introduction of more than 2% molybdenum leads to the release of the P-phase, and at a concentration of more than 5%, a secondary carbide of the M_6C type is formed. The tungsten content from 9 to 11% causes the appearance of both the P-phase and carbides of the M_6C type. These data are in good agreement with experimental data.

A comparative assessment of the calculated results obtained by the CALPHAD method and the experimental data obtained by the X-ray spectroscopy method has been carried out. The results obtained for determining the type and chemical composition of carbides are consistent with each other.

References

[1] O.M. Horst, D. Schmitz, J. Schreuer, P. Git, H. Wang, C. Körner, G. Eggeler, Thermoelastic properties and γ'-solvus temperatures of single-crystal Ni-base superalloys, Journal of Materials Science 56 (2021) 7637-7658. DOI: https://doi.org/10.1007/s10853-020-05628-w

[2] B. Chen, W.-P. Wu, M.-X. Chen, Orientation-Dependent Morphology and Evolution of Interfacial Dislocation Networks in Ni-Based Single-Crystal

Superalloys: A Molecular Dynamics Simulation, Acta Mechanica Solida Sinica 34 (2021) 79-90. DOI: https://doi.org/10.1007/s10338-020-00172-1

[3] M. Mazzarisi, S.L. Campanelli, A. Angelastro, F. Palano, M. Dassisti, In situ monitoring of direct laser metal deposition of a nickel-based superalloy using infrared thermography, The International Journal of Advanced Manufacturing Technology 112 (2021) 157-173. DOI: https://doi.org/10.1007/s00170-020-06344-0

[4] W. Song, X.-G. Wang, J.-G. Li, Y.-S. Huang, J. Meng, Y.-H. Yang, J.-L. Liu, J.-D. Liu, Y.-Z. Zhou, X.-F. Sun, Role of Ru on the Microstructural Evolution During Long-Term Aging of Ni-Based Single Crystal Superalloys, Acta Metallurgica Sinica (English Letters) 33 (2020) 1689-1698. DOI: https://doi.org/10.1007/s40195-020-01110-3

[5] O.I. Balyts'kyi, O.O. Krokhmal'nyi, Pitting corrosion of 12Kh18AG18Sh steel in chloride solutions, Materials Science 35 (1999) 389-394. DOI: https://doi.org/10.1007/BF02355483

[6] A. Borouni, A. Kermanpur, Effect of Ta/W Ratio on Microstructural Features and Segregation Patterns of the Single Crystal PWA1483 Ni-Based Superalloy, Journal of Materials Engineering and Performance 29 (2020) 7567-7586. DOI: https://doi.org/10.1007/s11665-020-05189-8

[7] S. Yang, J. Yun, C.-S. Seok, Rejuvenation of IN738LC gas-turbine blades using hot isostatic pressing and a series of heat treatments, Journal of Mechanical Science and Technology 34 (2020) 4605-4611. DOI: https://doi.org/10.1007/s12206-020-1018-2

[8] B. Yin, G. Xie, X. Jiang, S. Zhang, W. Zheng, L. Lou, Microstructural Instability of an Experimental Nickel-Based Single-Crystal Superalloy, Acta Metallurgica Sinica (English Letters) 33 (2020) 1433-1441. DOI: https://doi.org/10.1007/s40195-020-01057-5

[9] A. Pandey, K.J. Hemker, Temperature Dependence of the Anisotropy and Creep in a Single-Crystal Nickel Superalloy, JOM 67 (2015) 1617-1623. DOI: https://doi.org/10.1007/s11837-015-1414-8

[10] L. Chai, J. Huang, J. Hou, B. Lang, L, Wang, Effect of Holding Time on Microstructure and Properties of Transient Liquid-Phase-Bonded Joints of a Single Crystal Alloy, Journal of Materials Engineering and Performance 24 (2015) 2287-2293. DOI: https://doi.org/10.1007/s11665-015-1504-3

[11] A.A. Glotka, S.V. Gaiduk, Distribution of Alloying Elements in the Structure of Heat-Resistant Nickel Alloys in Secondary Carbides, Journal of Applied Spectroscopy 87 (2020) 812-819. DOI: https://doi.org/10.1007/s10812-020-01075-2

[12] O.I. Balyts'kyi, L.M. Ivas'kevych, V.M. Mochul's'kyi, Mechanical properties of martensitic steels in gaseous hydrogen, Strength of Materials 44 (2012) 64-71. DOI: https://doi.org/10.1007/s11223-012-9350-0

[13] C.Z. Zhu, R. Zhang, C.Y. Cui, Y.Z. Zhou, Y. Yuan, Z.S. Yu, X. Liu, X.F. Sun, Effect of Ta Addition on the Microstructure and Tensile Properties of a Ni-Co Base Superalloy, Metallurgical and Materials Transactions A 52 (2021) 108-118. DOI: https://doi.org/10.1007/s11661-020-06081-9

[14] S.A. Oh, R.E. Lim, J.W. Aroh, A.C. Chuang, B.J. Gould, J.V. Bernier, N. Parab, T. Sun, R.M. Suter, A.D. Rollett, Microscale Observation via High-Speed X-ray Diffraction of Alloy 718 During In Situ Laser Melting, JOM 73 (2021) 212-222. DOI: https://doi.org/10.1007/s11837-020-04481-1

[15] Y. Chen, H.M. Wang, Growth morphologies and mechanisms of non-equilibrium solidified MC carbide, Journal of Materials Research 21 (2006) 375-379. DOI: https://doi.org/10.1557/jmr.2006.0043

[16] Y.H. Kong, Q.Z. Chen, D.M. Knowles, Effects of minor additions on microstructure and creep performance of RR2086 SX superalloys, Journal of Materials Science 39 (2004) 6993-7001. DOI: https://doi.org/10.1023/B:JMSC.0000047543.64750.83

[17] S. Tin, T.M. Pollock, W. Murphy, Stabilization of thermosolutal convective instabilities in Ni-based single-crystal superalloys: Carbon additions and freckle formation, Metallurgical and Materials Transactions A 32 (2001) 1743-1753. DOI: https://doi.org/10.1007/s11661-001-0151-5

[18] N.V. Petrushin, E.M. Visik, M.A. Gorbovets, R.M. Nazarkin, Structure–phase characteristics and the mechanical properties of single-crystal nickel-based rhenium-containing superalloys with carbide–intermetallic hardening, Russian Metallurgy (Metally) 2016 (2016) 630-641. DOI: https://doi.org/10.1134/S0036029516070119

[19] O.I. Balyts'kyi, L.M. Ivas'kevych, J.J. Eliasz, Static Crack Resistance of Heat-Resistant KhN43MBTYu Nickel-Chromium Alloy in Gaseous Hydrogen, Strength of Materials 52 (2020) 386-397. DOI: https://doi.org/10.1007/s11223-020-00189-4

[20] Z. Yu, J. Qiang, J. Zhang, L. Liu, Microstructure evolution during heat treatment of superalloys loaded with different amounts of carbon, Journal of Materials Research 30 (2015) 2064-2072. DOI: https://doi.org/10.1557/jmr.2015.127

[21] G.D. Pigrova, A.I. Rybnikov, Carbide phases in a multicomponent superalloy Ni-Co-W-Cr-Ta-Re,

The Physics of Metals and Metallography 114 (2013) 593-595.
DOI: https://doi.org/10.1134/S0031918X13070089

[22] O.A. Glotka, Modelling the composition of carbides in nickel-based superalloys of directional crystallization Journal of Achievements in Materials and Manufacturing Engineering 102/1 (2020) 5-15. DOI: https://doi.org/10.5604/01.3001.0014.6324

[23] H. Ohtani, The CALPHAD Method, in: H. Czichos, T. Saito, L. Smith (eds.), Springer Handbook of Materials Measurement Methods, Springer Handbooks, Springer, Berlin, Heidelberg, 2006, 1001-1030. DOI: https://doi.org/10.1007/978-3-540-30300-8_20

[24] N. Saunders, U.K.Z. Guo, X. Li, A.P. Miodownik, J.-Ph. Schillé, Using JMatPro to model materials properties and behavior, JOM 55 (2003) 60-65. DOI: https://doi.org/10.1007/s11837-003-0013-2

[25] S. Xiang, S. Mao, Z. Shen, H. Long, H. Wei, S. Ma, J.X. Zhang, Y. Chen, J. Zhang, B. Zhang, Y. Liu, Site preference of metallic elements in $M_{23}C_6$ carbide in a Ni-based single crystal superalloy, Materials and Design 129 (2017) 9-14.
DOI: https://doi.org/10.1016/j.matdes.2017.05.023

[26] X.B. Hu, Y.L. Zhu, L.Z. Zhou, B. Wu, X.L. Ma, Atomic imaging of the interface between $M_{23}C_6$-type carbide and matrix in a long-term ageing polycrystalline Ni-based superalloy, Philosophical Magazine Letters 95/4 (2015) 237-244. DOI: https://doi.org/10.1080/09500839.2015.1039621

[27] R. Yong-Hua, G. Yong-Xiang, H.G. Xiang, Characterization of $M_{23}C_6$ carbide precipitated at grain boundaries in a superalloy, Metallography 22/1 (1989) 47-55.
DOI: https://doi.org/10.1016/0026-0800(89)90021-9

[28] A. Balitskii, Hydrogen assisted crack initiation and propagation in nickel-cobalt heat resistant superalloys, Procedia Structural Integrity 16 (2019) 134-140. DOI: https://doi.org/10.1016/j.prostr.2019.07.032

[29] O.A. Glotka, S.V. Haiduk, Distribution of elements in carbides of multicomponent Superalloys, Metallofizika i Noveishie Tekhnologii 42/6 (2020) 869-884 (in Russian).
DOI: https://doi.org/10.15407/mfint.42.06.0869

[30] A. Glotka, V. Ol'shanetskii, Prediction thermophysical characteristics heat-resistant nickel alloys directional crystallization, Acta Metallurgica Slovaca 27/2 (2021) 68-71.
DOI: https://doi.org/10.36547/ams.27.2.813